World Academy of Science, Engineering and Technology
International Journal of Electrical and Computer Engineering
Vol:15, No:5, 2021

Modelling of Multi-Agent Systems for the Scheduling of Multi-EV Charging from Power Limited Sources

Manan'Iarivo Rasolonjanahary, Chris Bingham, Nigel Schofield, Masoud Bazargan

***Abstract*—**This paper presents the research and application of model predictive scheduled charging of electric vehicles (EV) subject to limited available power resource. To focus on algorithm and operational characteristics, the EV interface to the source is modelled as a battery state equation during the charging operation. The researched methods allow for the priority scheduling of EV charging in a multi-vehicle regime and when subject to limited source power availability. Priority attribution for each connected EV is described. The validity of the developed methodology is shown through the simulation of different scenarios of charging operation of multiple connected EVs including non-scheduled and scheduled operation with various numbers of vehicles. Performance of the developed algorithms is also reported with the recommendation of the choice of suitable parameters.

***Keywords*—**Model predictive control, non-scheduled, power limited sources, scheduled and stop-start battery charging.

I. Introduction

EVs play an important role in the reduction of reliance on fossil-based fuels and the use of electrical energy from renewable sources. This trend for EV is demonstrated by the number of EV car models that manufacturers are now developing. However, the increasing share of renewable energy required from the power grid, particularly at a domestic level, requires the adoption of appropriate tools and measures such as energy storage and demand response to avoid power shortages (grid balancing). The charging process depends on the electrical characteristics of both the EV battery (state-of-charge, type, etc.) and the type of charging station EVSE (electric vehicle support equipment). The use of energy from renewable sources to simultaneously charge multiple EVs requires a control mechanism that can be achieved using multi-agent models [1] associated with Model Predictive Control (MPC) [2].

Most people charge their EV at home overnight using a domestic charge point. For domestic charging, the standard price varies between 14.3 p to 20 p per kWh; for off peak periods the range varies from 4.7 p to 12.2 p per kWh and for peak periods between 13.33 p to 19.91 p per kWh. Some charging costs from different energy providers are shown in Appendix, Table V. In general, two charging options exist: standard 3 kW or fast 7 kW charge points. The 7 kW charge point takes roughly half the charging time of the 3 kW but costs more to install.

The adoption of multi-agent systems allows the determination of a charging schedule for each EV in a multi-vehicle system based on consideration of their priority (possibly based on a tariff system). According to the charge point rate, the available charging current is about 30 A. However, a maximum available current of I_{lim} (= 200 A) is used in this study to speed up the calculation.

Here then, the application of a control mechanism for multi-EV charging is proposed that accommodates current state of charge of each EV and priority scheduling.

M. I. L. Rasolonjanahary and C. Bingham are with the School of Engineering, University of Lincoln, Brayford Pool, Lincoln LN6 7TS, UK (e-mail: 17687516@students.lincoln.ac.uk, e-mail: cbingham@lincoln.ac.uk)

N. Schofield is now with the School of Computing and Engineering, University of Huddersfield, Huddersfield HD1 3DH, UK (e-mail: n.schofield@hud.ac.uk).

M. Bazargan is with Power Technologies Limited, Upper Reule Cottage, Newport Road, Haughton, Stafford ST18 9JH, UK (e-mail: masoud.bazargan@powertechnologieslimited.com).

II. Formulation and Methodology

MPC has become an important advanced control technique for applications where unaccommodated hard- and soft-constraints could readily make more traditional multivariable feedback systems impart closed loop instability [3]-[5]. It has been successfully applied to many industrial control systems e.g., [6], [7].

Compared to alternative multivariable techniques, MPC has a number of advantages for multi-EV charge scheduling:

1) Formulation of the constrained optimisation problem as a quadratic function;
2) Allowance for the plant model in the optimisation;
3) Multiple inputs, multiple outputs are readily incorporated;
4) Allowance for multiple equality and inequality constraints.

A. Problem Formulation

A solution for the sharing of a current-limited power source for charging n EVs in a small carpark or a domestic estate can be solved by minimising a quadratic cost function J:

$$J(v,I)=\frac{1}{2}\sum_{k=1}^{M}\left\|v(k)-v_{ref}(k)\right\|_{Q}^{2}+\left\|I(k)-I(k-1)\right\|_{R}^{2} \quad (1)$$

where $v(v_1, v_2, v_3, \ldots, v_n)$ and $I(I_1, I_2, I_3, \ldots, I_n)$ represent, respectively, the voltage and charging current of each battery, subject to input constraints (considered below). Using MPC terminology, v is the set of states and I is the set of manipulated variables. In (1), R and Q are symmetric and

positive definite matrices denoting, respectively, relatively 'weights' of input and output priorities. A basic model of multiple EV sharing can be obtained by assuming their batteries to appear as capacitive loads, and are collectively subject to a maximum total charging current constraint, as described by (2) and (3) for the simplified case of 3 EVs:

$$\frac{d}{dt}\begin{bmatrix} v_1 \\ v_2 \\ v_3 \end{bmatrix} = \begin{bmatrix} -\frac{1}{r_1 C_1} & 0 & 0 \\ 0 & -\frac{1}{r_2 C_2} & 0 \\ 0 & 0 & -\frac{1}{r_3 C_3} \end{bmatrix} \begin{bmatrix} v_1 \\ v_2 \\ v_3 \end{bmatrix} + \begin{bmatrix} \frac{1}{C_1} & 0 & 0 \\ 0 & \frac{1}{C_2} & 0 \\ 0 & 0 & \frac{1}{C_3} \end{bmatrix} \begin{bmatrix} I_1 \\ I_2 \\ I_3 \end{bmatrix} \quad (2)$$

and,

$$I_1 + I_2 + I_3 \le I_{\lim} \quad (3)$$

In the formation of MPC, both the dynamic model (2) and the current limits (3) are considered as constraints on the optimisation of the cost function (1)–see Fig. 1 for the underlying isolated battery model where C represents the equivalent capacitance of the battery and r specifies its bulk internal leakage. For this study, the battery is assumed to incur very small leakage in line with modern cells, and so r is taken to be 100 kΩ. For each battery, the capacitance value is derived from the energy capacity of the car's battery using (4), where E is the rated energy capacity measured in Joules (J), and for simplicity it is assumed that the initial terminal voltage of the battery (assumed to be related to State of Charge (SoC)) is half that of a nominal fully charged battery V_{ref} at the start of the scheduled charging trials—although it should be noted that this is completely arbitrary.

$$C = \frac{8E}{3V_{ref}^2} \quad (4)$$

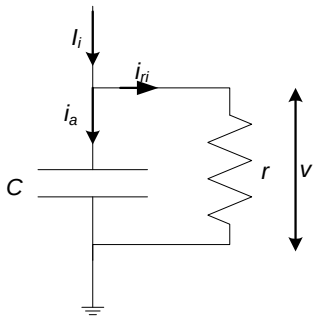

Fig. 1 Analogic EV battery model

B. Methodology

The solution (1) can be achieved through numerically solving the constrained optimization problem using a receding horizon approach [2]:

1) At time k and for the current state $v(k)$, solve, on-line, an open-loop optimal control problem over some future interval of length M taking into account the current and future constraints—M is the length of receding horizon,
2) Apply the first step in the resulting optimal control sequence to the plant, and
3) Repeat the procedure at time $(k+1)$ using the current state $v(k+1)$.
4) Perform the following steps at each iteration [2]:

- Measure the system outputs and inputs.
- Estimate the present state of the system.
- Calculate the next control move by solving (1) and applying the resulting control actuation (a current demand in the case of charging EVs).

Fig. 2 shows the representation of three cars during the charging process.

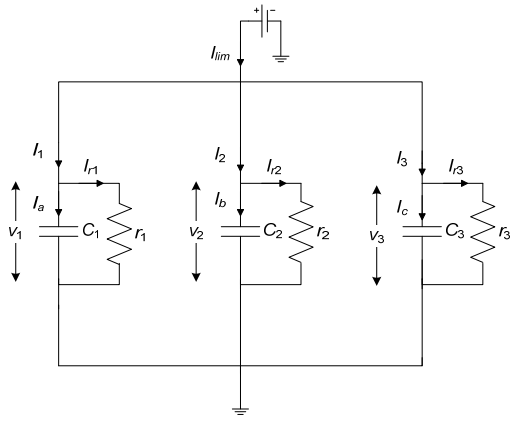

Fig. 2 Multi-agent model with three EVs

C. Priority Attributions

For UK public charging sites, the price for charging an EV could be twice that of a domestic counterpart (e.g., 39 p per kWh has been quoted)—example charging costs from different public network providers are shown in Appendix, Table VI. The price shown depends on the type of charger. Although there are more than 10,000 charging sites now in the UK, the rapid adoption of EVs could mean long queues for charge, or a stagnation of the market if the number charging capacity does not increase with the number of EVs on the road. An interim solution is to introduce an integrated priority scheduling for charging (a first come, first serve option may not be appropriate if the first EV arriving requires 100% charge with a large EV battery capacity). Two charging priorities are proposed, although a combination of each will likely be a preferred solution. First, on price, the customer who wants to be charged the fastest has to pay more for using more of the constrained resource. Secondly, on the level of required charging, the customer who requires only a small amount of top-up charge can be given a short-term priority. This could avoid space utilisation issues on constrained sites.

In this paper, the element of the priority matrix Q could be expressed as proportional to the matrix price P per kWh the customer is willing to pay and inversely proportional to the square of the matrix level L (kWh) which represents the level of charge required. Both P and L are diagonal matrices. In short, Q is defined by:

$$[Q]=[P][L]^{-2} \quad (5)$$

III. Case Study

Different scenarios of charging operation of multiple EV are now considered through the use of simulation trials, including a (benchmark) non-scheduled solution with unlimited power resource, and a scheduled solution with a constrained maximum available current of I_{lim} (= 200 A). Initial studies are constrained to a 3-EV system viz. a Tesla S, Jaguar I-Pace and Nissan Leaf, represented by their respective battery models (with associated energy capacities—see Fig. 3). The terminal battery voltage and current of each EV battery is monitored. Max_{IT}, Max_{IJ} and Max_{IN} represent the maximum charging currents for Tesla S, Jaguar I-Pace and Nissan Leaf, respectively (taken from vehicle specifications shown in Appendix, Table IV), and V_{Tref}, V_{Jref} and V_{Nref} specify the desired battery terminal voltages (related to SoC) for Tesla S, Jaguar I-Pace and Nissan Leaf models, respectively.

The parameters are summarized in Table I along with their maximum assumed charging currents. The parameters of the MPC simulations are summarised in Table II. The initial charging current for all three vehicles is 0 A. All EVs are fed from an AC 3-phase rectified voltage source giving a nominal 600 V DC source voltage in this case: Note, since current control is being used to control the charging of the vehicles, the input source voltage does not affect the scheduling regime from a control and performance perspective in this instance.

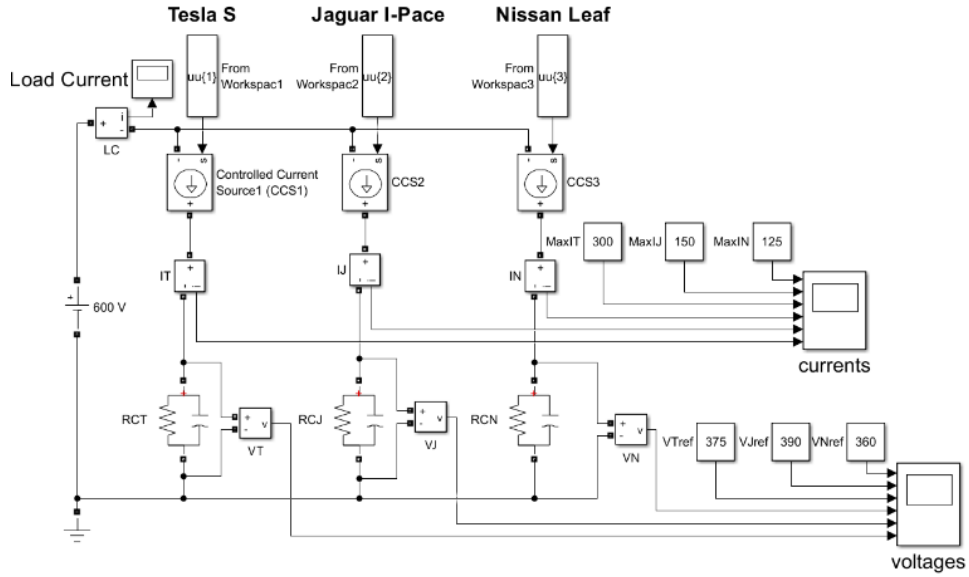

Fig. 3 Circuit model containing a voltage source on the left-hand side for three cars

TABLE I
Vehicle Data

Car models	Battery capacity (kWh)	Nominal voltage (V)	Maximum charging current (A)	Capacitance (F)	Resistance (kΩ)
Tesla S	100	375	300	6827	100
Jaguar I-Pace	90	390	150	5680	100
Nissan Leaf	62	360	125	4593	100

TABLE II
MPC Simulation Parameters

Sample time (s)	15
Control Horizon (number of manipulated variables moves to be optimized at control interval *k*)	10
Prediction Horizon (number of future control intervals the MPC controller must evaluate by prediction when optimizing its manipulated variable at control interval *k*)	10

A. Non-Scheduled Scenario

In this case, the results consisting of the voltages and currents during the charging process are shown in Fig. 4. They are charged simultaneously without any priority and with unlimited power resource. The charging dynamics depend on the initial terminal voltage and capacity of each battery. The dashed lines in Fig. 4 A correspond to the nominal desired terminal for each vehicle. The dashed profiles in Fig. 4 B denote the maximum charging currents for each vehicle model.

The Tesla S model reaches its reference voltage of 375 V first in 1.19 hours. This is followed by the Nissan Leaf model with a voltage reference of 360 V in 1.84 hours. For the Jaguar I-Pace model, 2.06 hours is required to be fully charged. The overall time to charge the three cars is therefore 2.06 hours (the constraint (3) is not active in this scenario).

Notably, it can be seen that the maximum current required from the supply is 575 A.

B. Scheduled Scenario with Constraint Power Source (200 A max)

This scenario has been simulated with a diagonal matrix Q = (8, 1, 2). These entries represent, respectively, the priority coefficient for Tesla S, Jaguar I-Pace and Nissan Leaf models, and so in this case the Tesla S has been given greater priority

for its charging requirements. Moreover, the results are shown in Fig. 5.

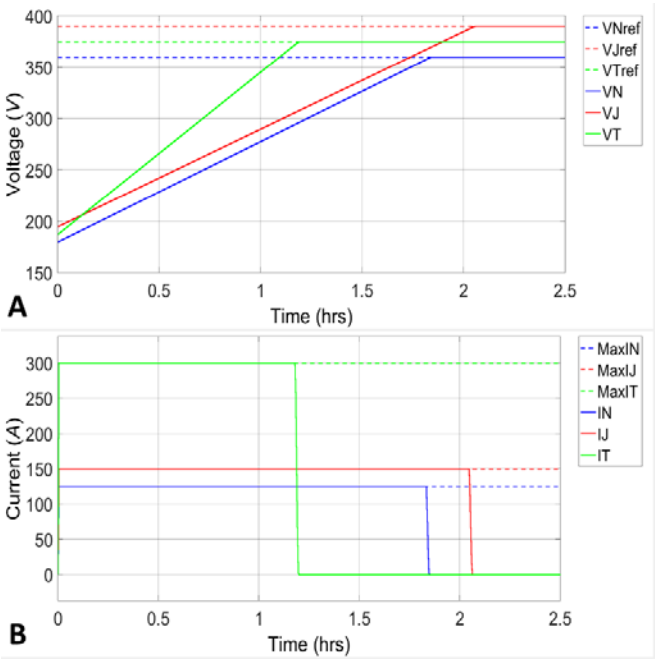

Fig. 4 Voltages and currents of the EV with unscheduled charging (A) battery terminal voltage (B) battery current

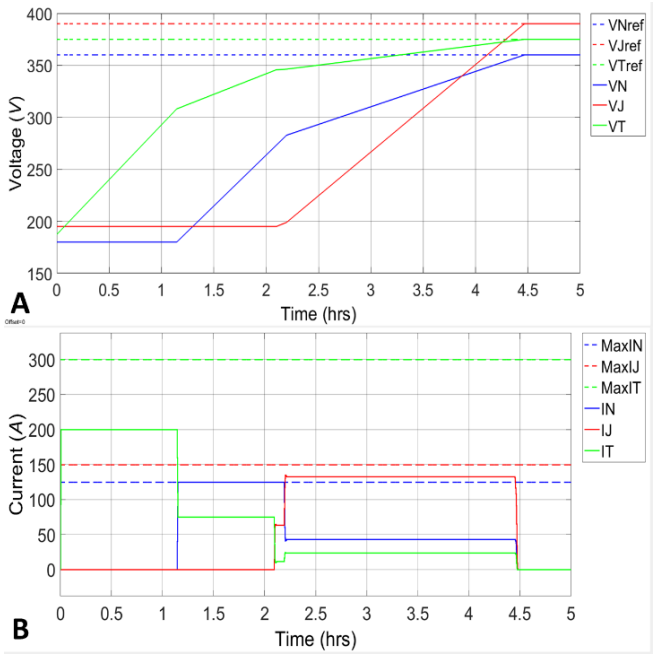

Fig. 5 Voltages and currents of the EV with scheduled priority charging Q = (8, 1, 2) (A) battery terminal voltage (B) battery current

The Tesla S model immediately begins charging due to its higher assigned priority with the maximum charging current being 200 A (see Fig. 5 B). The other two vehicles do not begin charging immediately in this instance. Only after t = 1.15 hours the Nissan Leaf begins to charge with a maximum current of 125 A, and the Tesla S keeps charging but at a lower current value of 75 A. The Jaguar I-Pace eventually begins sharing with a current of 63.53 A at ~2.1 hours. It can be seen that the apportioning of the limited current resource (200 A) changes throughout the charging period with all cars attaining their desired charge after 4.47 hours, but notably the Tesla S is allowed greater charge during the early part of the regime in case it needs to become operational (driven away) earlier—even greater emphasis given by the Q matrix would mean that the Tesla S could be fully charged prior to the others starting any significant charging. This trial clearly demonstrates the viability of such a priority scheduling technique using MPC.

C. Ad-Hoc Stop-Start Charging and Vehicle Arrival Departure

This scenario involving four EVs considers their arrival and departure at a charging point. At t = 0, a Tesla S arrives and begins to charge its battery using the maximum charging current value of 200 A. At t = 1.78 hours, it finishes its charging and departs. This is shown by the level of its charging current reduced to zero, Fig. 6 B. At the same time a second car, Nissan Leaf, enters the charging point and starts its operation with its maximum charging current of 125 A. At t = 2.72 hours, a third car, Jaguar I-Pace, comes to this charging point and draws 75 A to charge its battery. At t = 3.8 hours, a fourth car, Citroën C-Zero, arrives at the charging point but it must wait until t = 4.1 hours to charge its battery. From this time, the previous two cars have their battery voltages close to their respective references. Hence, their charging currents decrease allowing the Citroën C-Zero to commence its charging process. At t = 5.14 hours, the charging operations of the three cars are complete. The EV battery voltages and currents drawn during the timeline of charging process is shown in Fig. 6. This scenario is simulated using the priority scheduling with matrix Q = (1000, 1, 2, 0.1) for the four vehicles.

Next, a similar scenario with the same four vehicles is considered but an ad-hoc starting and stopping of charging of some vehicles are investigated. This might occur when there is insufficient power to charge all vehicles and so the charging of some can be temporarily interrupted (load shedding) and resumed later, or some cars may disconnect early to continue on their journeys and other vehicles arrive for charging. To investigate the flexibility of the algorithm to cater for such scenarios, a basic trial using the matrix Q = (8, 1, 2, 0.1) for the four vehicles is undertaken. The priorities of the Tesla S and Citroën C-Zero are interchanged at t = 1.33 hours i.e. the matrix Q becomes Q_1 = (0.1, 1, 2, 8). The results of the simulation are shown in Fig. 7.

Fig. 7 shows that the Tesla S is forced to stop charging for some time when it reaches 85% of its desired voltage at t = 1.33 hours (Fig. 7 A, black arrow)—effectively it could have disconnected and resumed its onward journey. This charging interruption allows the Citroën C-Zero to begin charging at its maximum current of 110 A. The Nissan Leaf begins to charge its battery at t = 1.15 hours. Its charging is now forced to interrupt at t = 1.33 hours while the Citroën C-Zero starts its

charging operation. The Nissan Leaf and Tesla S are then forced to resume charging respectively at t = 1.82 and 4.64 hours, mimicking what might occur if two vehicles arrived to begin charging (albeit this trial shows that the battery voltage has not deviated in this instance, but this is arbitrary). The Jaguar I-Pace commences to charge its battery at t = 2.58 hours. The overall charging process takes 5.32 hours.

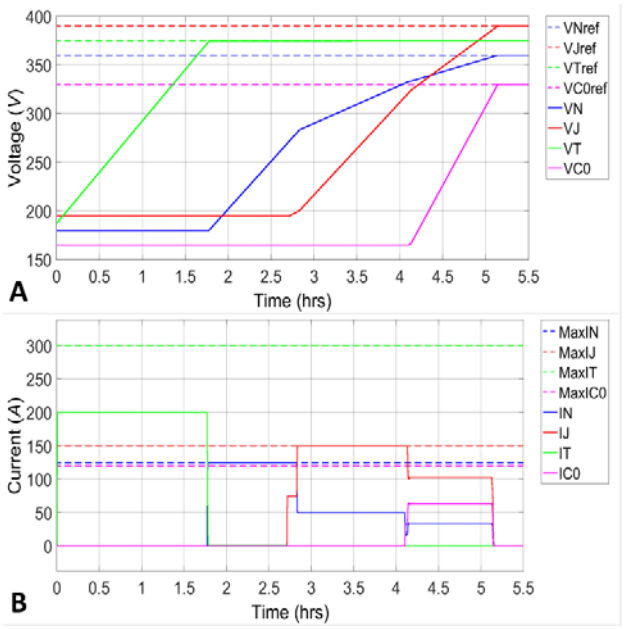

Fig. 6 Voltages and currents of the EV with scheduled priority charging of four vehicles with ad-hoc on-off charging (A) battery terminal voltage (B) battery current

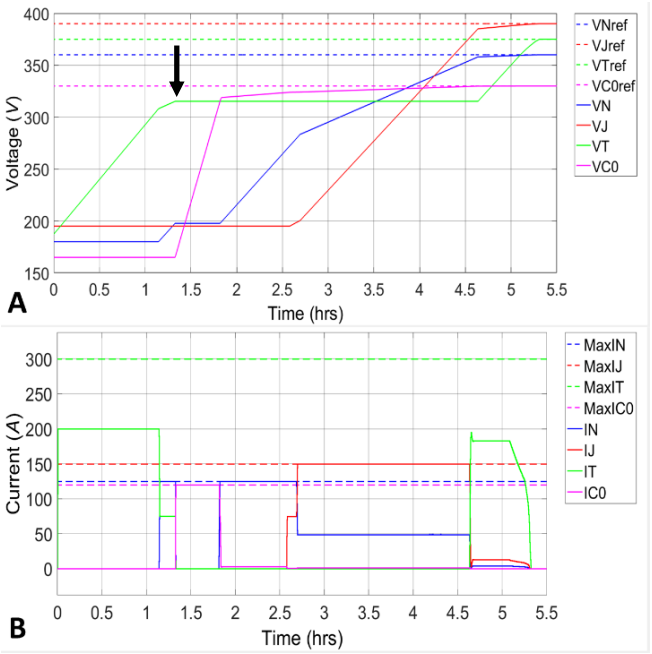

Fig. 7 Voltages and currents of the EV with scheduled priority charging of four vehicles with ad-hoc on-off charging (A) battery terminal voltage (B) battery current

D. Expansion to Greater Numbers of Vehicles

For completeness, the algorithm can be readily extended to operate with many more vehicles, albeit with an increase in computational load—see Section III *E*. In this case, 10 vehicles are considered.

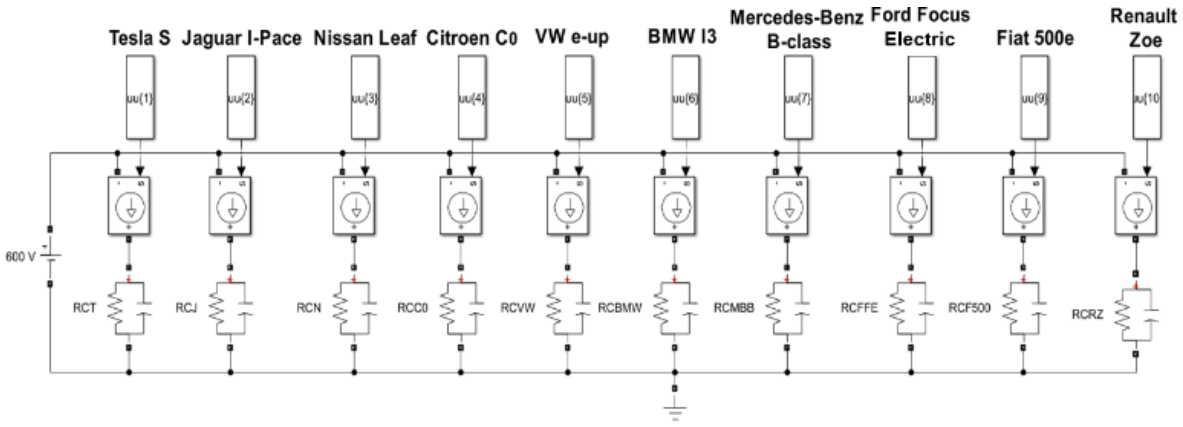

Fig. 8 Dynamic charging of ten vehicles

The 10 vehicles considered here are the Tesla S, Jaguar I-Pace, Nissan Leaf, Citroën C-Zero, VW e-up, BMW i3, Mercedes-Benz B-Class Electric, Ford Focus Electric, Fiat 500e and Renault Zoe. The priority matrix is taken as Q = (200, 44, 100, 2, 5, 0.02, 38, 1, 0.1, 0.01). First, a trial with no ad-hoc charge switching is undertaken, the results are shown in Fig. 9. During the entire process, the maximum available charging current is constrained to be 200 A.

Fig. 9 shows that the Tesla S model starts to charge its battery with a maximum value of 200 A. The Nissan Leaf, Jaguar I-Pace, Mercedes-Benz B-class Electric, VW e-up, Citroën C-Zero, Ford Focus Electric, Fiat 500e, BWM i3 and Renault Zoe models begin to charge their battery at t = 0.51, 2, 2.87, 3.53, 4.9, 5.57, 6.27, 6.76 and 7.3 hours, respectively. At t = 7.3 hours, all 10 cars charge their batteries simultaneously their battery without exceeding the maximum charging current of 200 A. All 10 cars will take 8.86 hours to

fully charge their batteries. This is around double the time compared to the cases for the three- and four-car models whose durations are 4.5 and 5.1 hours, respectively. Next, we want to see the case when some vehicles start and stop charging in an ad-hoc manner.

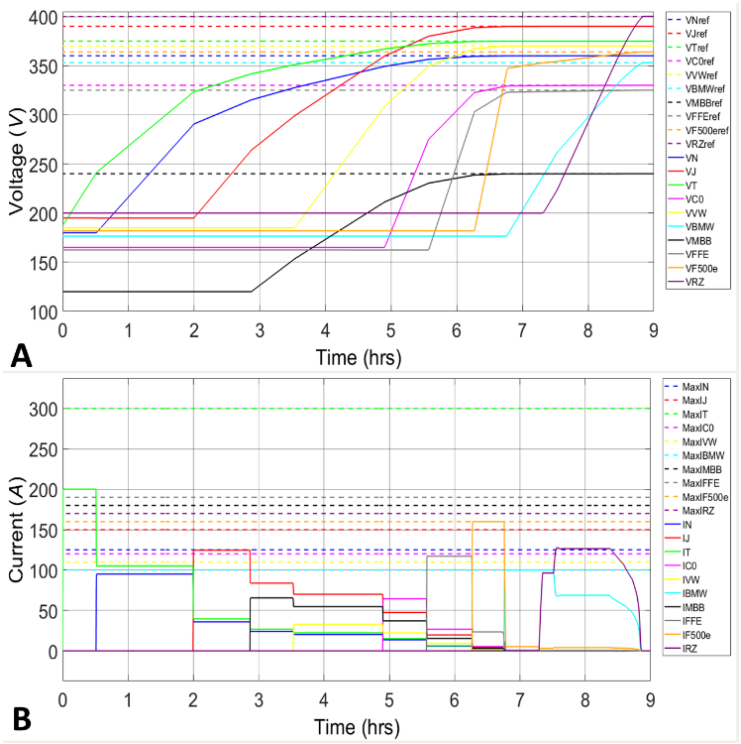

Fig. 9 Voltages and currents of the EV with scheduled priority charging of ten vehicles (A) battery terminal voltage (B) battery current

Fig. 10 shows that two cars (Nissan Leaf and Tesla S, blue arrow) have interrupted their charging process at t = 1.25 hours. At this time, the Q_1 matrix is chosen to be Q_1 = (0.01, 0.1, 0.02, 5, 2, 100, 1, 38, 44, 200). Thus, the Renault Zoe (priority coefficient (PC) of 200), BMW i3 (PC = 100), Fiat 500e (PC = 44) and Ford Focus Electric (PC = 38) begin charging their battery at t = 1.25, 1.79, 1.95 and 2.49 hours, respectively. At t = 2.9 hours, four cars (BMW i3, Ford Focus Electric, Fiat 500 and Renault Zoe, red arrow) have stopped temporarily charging their battery. The Q_2 matrix, at this point, is Q_2 = (0.01, 0.02, 5, 0.1, 200, 44, 1, 100, 2, 38). The VW e-up (PC = 200) commences to charge its battery at t = 2.9 hours. The Ford Focus Electric (PC = 100), BMW i3 (PC = 44), Renault Zoe (PC = 38), Nissan Leaf (PC = 5) and Fiat 500e (PC = 2) resume their charging at t = 3.37, 3.72, 4.05, 4.28 and 4.53 hours, respectively. At t = 5.12 hours, another set of cars have suspended their charging process (green arrow). The new Q_3 = (2, 5, 38, 200, 0.01, 1, 100, 0.1, 44, 0.02). The Citroën C-Zero (PC = 200) commences to charge its battery at t = 5.12 hours. The Mercedes Benz B-class Electric (priority coefficient of 1) starts its charging process at t = 5.6 hours. The Fiat 500e (PC = 44) and Nissan Leaf (PC = 38) recharge their battery at t = 6.13 and 6.38 hours, respectively. The Jaguar I-Pace begins to charge its battery at t = 6.58 hours. The Tesla S (PC = 2), BMW i3 (PC = 1), Ford Focus Electric (PC = 0.1), Renault Zoe (PC = 0.02) and VW e-up (PC = 0.01) recommence charging their batteries at t = 8.28, 9.42, 9.47, 9.474 and 9.51 hours, respectively. The overall charging time has taken 9.51 hours.

E. Computational Performance

The MPC depends on the control horizon parameter M and is an important parameter for determining how long the algorithm takes to execute at each sampling instant. For this purpose, the number of EVs being charged is increased to six (the three additional cars are Citroën C-Zero, VW e-up and BMW i3). Their respective data are given in Table III. Calculation times are calculated by varying the control horizon M. The results are normalised with respect to the execution time corresponding to M = 50, as shown in Fig. 11.

TABLE III
ADDITIONAL CAR DATA

Car models	Battery capacity (kWh)	Nominal voltage (V)	Capacitance (F)	Maximum charging current (A)
Citroën C-Zero	16	330	1410	120
VW e-up	18.7	370	1311	110
BMW i3	42.2	360	3125	100

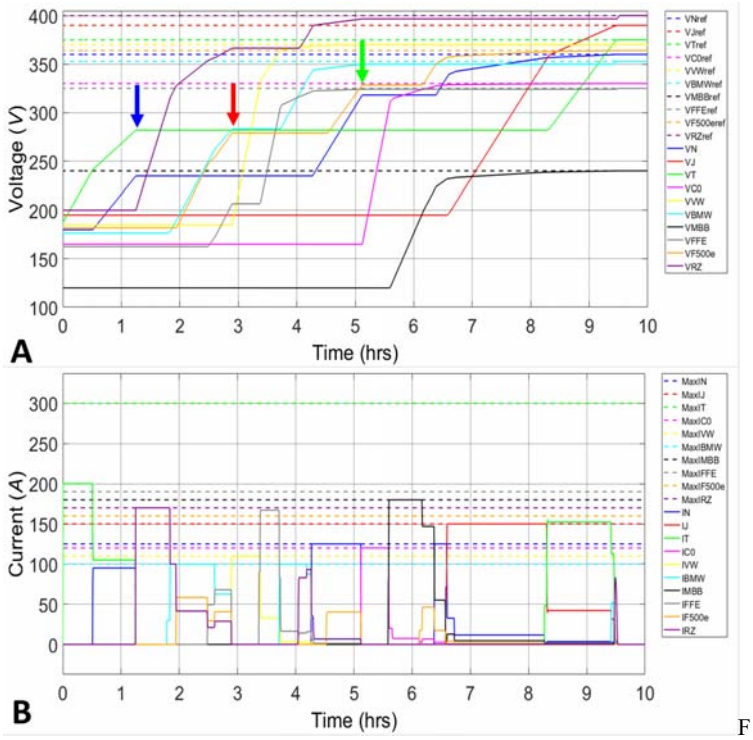

Fig. 10 Voltages and currents of the EV with scheduled priority charging of ten vehicles with ad-hoc on-off charging (A) battery terminal voltage (B) battery current

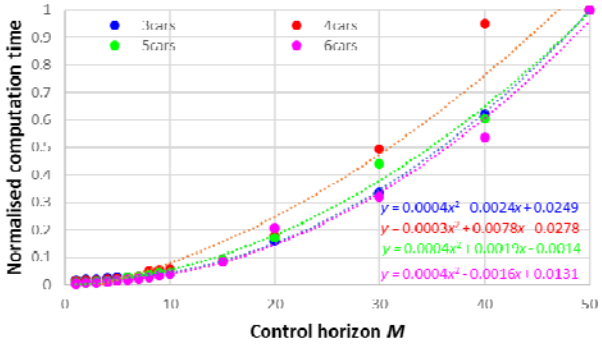

Fig. 11 Computation time vs. control horizon *M*

Fig. 11 shows that the normalised simulation time, for all cases, increases quadratically with the control horizon *M* and so care needs to be taken when selecting *M* particularly as the number of vehicles increases.

IV. Conclusion

A method of control of charging process of EVs has been developed using a MPC algorithm. Each vehicle is represented by a battery modelled consisting of a capacitor in parallel with a leakage resistor. The MPC method optimises a quadratic cost function involving the priority scheduling of each vehicle and its desired battery voltage, and subject to a constrained power resource. Different charging scenarios have been presented including a comparison of non-scheduled and scheduled charging with various numbers of vehicles and constrained current resource. These results have shown the validity of the presented methodology as a candidate technique for the dynamic apportioning of a scarce resource (power) for the ad-hoc charging of multiple EVs. A limitation to its use could be the computational effort required, as this is shown to increase quadratically with the control horizon and the number of vehicles.

Appendix

TABLE IV
EV Battery Parameters

Car models	Battery Voltage (V)	Battery Capacity (kWh)
BMW i3	360	42 [8]
Fiat 500e	364	24 [8]
Mercedes-Benz B-Class Electric	240	28 [8]
Renault Zoe	400	22/52 [9]
VW e-up	374	18.7 [10]
Jaguar	390	90 [11]
Citroën C-Zero	330	16 [12]
Ford Focus Electric	325	23 [12]

TABLE V
Domestic Charging [13]

Name	Standard (p/kWh)	Off-peak (p/kWh)	Peak (p/kWh)
British Gas	20	4.7	Not available
EDF	14.34	9	19.91
Eon	19.8	10.44	17.19
Good energy	16.27	12.2	16.34
Ovo energy	15.89	10.33	17.78
Octopus Energy	Not available	5	13.33
Scottish Power	17.81	4.74	Not available
Shell Energy	15.5	Not available	Not available

TABLE VI
PUBLIC CHARGING SITES [14]

Name	Standard (p/kWh)
Ecotricity	30
GeniePoint	30
Instavolt	35
Shell Recharge	39
Tesla	25
Ubitricity	24

ACKNOWLEDGMENT

The research is undertaken with the support of Smart Energy Network Demonstrator (SEND) and Keele University.

REFERENCES

[1] S. Ohtani, Y. Shirasawa, O. Mori and J. Kawaguchi, "Power-Peak-Curbing Switching Schedule for a Multiagent System," *Transactions of the Japan Society for Aeronautical and Space Sciences, Aerospace Technology Japan*, vol. 14, 2016, pp. 25-30
[2] A. Bemporad, M. Morari, and N. L Ricker, *Model Predictive Control Toolbox,* 2005.
[3] D. E. Seborg, *Process Dynamics and Control*, John Wiley & Sons, Incorporated, 2012.
[4] J. Currie, A. Prince-Pike, and D. I. Wilson, "Auto-code generation for fast embedded Model Predictive Controllers," in *19th International Conference on Mechatronics and Machine Vision in Practice (M2VIP),* 2012, pp. 116-122.
[5] A. Jain, F. Smarra, M. Behl, and R. Mangharam, "Data-Driven Model Predictive Control with Regression Trees—An Application to Building Energy Management," ACM Trans. Cyber-Phys. Syst., vol. 2, p. Article 4, 2018.
[6] S. Strand and J. R. Sagli, "MPC in Statoil – Advantages with In-House Technology," *IFAC Proceedings Volumes,* vol. 37, 2004, pp. 97-103.
[7] T. Geyer, G. Papafotiou, and M. Morari, "Model Predictive Control in Power Electronics: A Hybrid Systems Approach," in *Proceedings of the 44th IEEE Conference on Decision and Control,* 2005, pp. 5606-5611.
[8] https://batteryuniversity.com/learn/article/electric_vehicle_ev(dated 19/03/20
[9] https://www.evspecifications.com/ (dated 19/03/20)
[10] https://www.evspecifications.com/en/model/e4f07b (dated 19/03/20)
[11] https://autotechreview.com/technology/propulsion-system-of-the-new-jaguar-i-pace (dated 19/03/20)
[12] https://ev-database.uk/ (dated 20/03/20)
[13] https://www.zap-map.com/charge-points/ev-energy-tariffs/ (03/12/20)
[14] http://www.zap.map.com/charge-point/public-charging-point-networks/ (dated 03/12/20)